Available online at www.sciencedirect.com
ScienceDirect
Trans. Nonferrous Met. Soc. China 19(2009) 40−44
Transactions of Nonferrous Metals Society of China
www.tnmsc.cn

Microstructure and corrosion behavior of Mg-Sn-Ca alloys after extrusion

T. ABU LEIL[1], N. HORT[1], W. DIETZEL[1], C. BLAWERT[1], Y. HUANG[1], K. U. KAINER[1], K. P. RAO[2]

1. GKSS Forschungszentrum Geesthacht GmbH; Max-Planck Strasse 1, Geesthacht 21502, Germany;
2. City University of Hong Kong, 83 Tat Chee Avenue, Kowloon, Hong Kong

Received 27 May 2008; accepted 24 December 2008

Abstract: Mg-Sn-Ca alloys promise a reasonable corrosion resistance in combination with good creep resistance, likely due to the presence of $Ca_{2-x}Mg_xSn$ and other phases. The selected alloys with 3% Sn and Ca in the range of 1%−2% have been extruded in order to achieve more homogeneous microstructure compared with the as-cast alloys. Optical microscopy(OM) and X-ray diffraction(XRD) techniques were used to study the microstructure and phases of these alloys. The corrosion behavior of these alloys was investigated by means of salt spray test and potentio-dynamic measurements. The results obtained on the alloys Mg-3Sn (T3), Mg-3Sn-1Ca (TX31), and Mg-3Sn-2Ca (TX32) indicate the presence of the same phases in as-cast and after extrusion, namely Mg_2Sn, $Ca_{2-x}Mg_xSn$, and $Ca_{2-x}Mg_xSn/Mg_2Ca$, respectively. However, due to the occurrence of extensive recrystallization in the extrusion process, the grain size has significantly reduced after extrusion. The reduction leads to the improvement of the corrosion resistance after extrusion which is then comparable with the commercial alloy AZ91D.
Key words: magnesium-tin alloys; microstructure; corrosion; extrusion

1 Introduction

Magnesium alloys exhibit attractive property combinations of low densities and high specific strength. Therefore, they are gaining more significance and acceptance in various industries especially in automotive industry[1−2]. Replacing aluminum components with even lighter magnesium parts in automotive application results in reduced fuel consumption and therefore causing less environmental pollution[3]. The application area of these alloys is narrow in industry; confined to parts such as steering wheels, column supports, roof frames, and gear box housings. The highly essential and favored alloys currently in use are based on Mg-Al system, such as AZ or AM series alloys. They offer advantages like good corrosion resistance, good castability and suitable property profile at competitive costs. However, due to their poor creep resistance at elevated temperatures, they cannot be directly used for the fabrication of an engine block[4−5]. The discontinuous precipitations of the $Mg_{17}Al_{12}$ phase at grain boundaries decrease the creep resistance[6]. Therefore, there is a clear need for the development of new magnesium alloys with an optimal combination of creep and corrosion resistance[4−10].

Recently, the alloy AJ62 has been successfully introduced for engine block applications. In this alloy system, Al_4Sr and $Mg_{13}Al_3Sr$ intermetallic phases improve the creep performance due to their stability at elevated temperatures. However, very specific conditions are required in order to use die casting for this alloy [8−10]. Other attempts to develop new magnesium alloys have been undertaken. In recent years, significant improvements on the binary Mg-Sn and ternary Mg-Sn-Ca system, in as-cast condition, have also been taken up for the purpose of achieving best combination of castability, creep and corrosion resistance[11−23]. Investigations on the Mg_2Sn phase or on the Mg_2Sn, Mg_2Ca, and $Ca_{2-x}Mg_xSn$ phases that can be formed in binary Mg-Sn or in ternary Mg-Sn-Ca alloys have been performed as well. It is also known that tin has a low melting point[24], and it is a comparatively economical metal to use. Furthermore, tin has a reputation of enhancing castability and is beneficial to providing corrosion resistance as well[25]. The addition of Ca has been found to improve the creep resistance[26]. In this work, the selected alloys, namely, Mg-3Sn (T3), Mg-3Sn-1Ca (TX31), and Mg-3Sn-2Ca (TX32) (mass fraction, %) have been investigated after extrusion. The

Corresponding author: T. ABU LEIL; Tel: +49-(0)4152/87-1966; Fax: +49-(0)4152/87-1909; E-mail: tarek.abuleil@gkss.de
DOI: 10.1016/S1003-6326(08)60225-3

microstructure has been characterized using optical microscopy. The corrosion behavior of these alloys has been investigated by means of salt spray test and potentio-dynamic polarization measurements. The influence of extrusion on the microstructure and corrosion resistance of these alloys has been examined and compared with the same alloys before extrusion.

2 Experimental

One binary Mg-3Sn and two ternary Mg-3Sn-*x*Ca alloys (*x*=1, 2, mass fraction, %) have been used. Their nominal compositions are given in Table 1. The investigated alloys were prepared using elemental metals with purities of 99.9% Mg (Hydro Magnesium, Norway), 99.9% Sn (MCP HEK, Germany), and 99.5% Ca (Merck, Germany). These alloys were prepared using induction furnace (Nabertherm, Germany) at approximately 720 ℃ under the shielding of Argon + SF_6 mixed cover gas, followed by gravity casting of the melt in permanent molds preheated to 200 ℃ to obtain cylindrical billets of 100 mm in diameter and 350 mm in length.

Table 1 Nominal compositions of three selected alloys

Alloy	Abbreviation	*w*/%		
		Sn	Ca	Mg
Mg-3Sn	T3	3	0	Bal.
Mg-3Sn-1Ca	TX31	3	1	Bal.
Mg-3Sn-2Ca	TX32	3	2	Bal.

The as-cast billets of the selected alloys were machined to 93 mm in diameter and 300 mm in length, and heat-treated for 6 h at 500 ℃. Indirect extrusion was carried out to produce round bars measuring 17 mm in diameter. The extrusion ratio was 1:30 and the extrusion rate (speed of the extruded bar at die exit) was set to 10 m/min (corresponding ram speed set at about 5.5 mm/s) at an extrusion temperature of 350 ℃.

Round discs about 4 mm in thickness and 17 mm in diameter were used to examine the microstructure and the corrosion properties of these alloys. To study the microstructure, optical microscopy was used. The specimens were ground with silicon carbide paper to 4000 grit, and then polished with diamond paste (6 μm and 1 μm), respectively. Then, they were polished with OPS^{TM} suspension. These samples were further etched in a solution of 8 g picric acid, 5 mL acetic acid, 10 mL distilled water and 100 mL ethanol for 10 s. Finally, they were washed using ethanol and then blow-dried. The optical microscopy was performed on Reichert-Jung MeF3 microscope attached with digital camera. The microscope is connected with a computer to get digital image of the samples.

Similar specimens were ground with a 1200 grade silicone carbide paper and then cleaned with alcohol and dried for study by X-ray diffractometry(XRD). The phase identification was done using XRD by means of Siemens diffractometer operating at 40 kV and 40 mA with Cu K_α radiation. The measurements were conducted by step scanning (2θ) from 20° to 120° with a step size of 0.02°. A count time of 3 s per step was applied.

Two kinds of corrosion tests were performed, namely, polarization and salt spray test. For the polarization test the specimens were ground on one side, while the pre-requisite for the salt spray test is specimen ground on both sides. The potentio-dynamic polarization measurements were conducted for these alloys at room temperature, in a 5% NaCl solution with a pH value adjusted to 11 with NaOH. The measurements were performed in a standard three electrode set-up with the specimens of various alloys as working electrodes (exposed area of 1.54 cm^2 in contact with the electrolyte) in conjunction with an Ag/AgCl reference electrode and a platinum counter electrode. After recording the free corrosion potential for 30 min, the polarization scan was started at −250 mV relative to the free corrosion potential with a scan rate of 0.2 mV/s. The corrosion rate was calculated using the current determined from the intersection of the cathodic Tafel slope with the vertical through the free corrosion potential. The temperature of the salt spray chamber was controlled at 35 ℃. The specimens were exposed to salt spray of 5% NaCl solution (pH value 7) for 48 h. After the test, the corroded specimens were rinsed with water and cleaned in chromic acid to remove the oxides and dried subsequently. The mass loss of the specimens was used to calculate the average corrosion rate.

3 Results and discussion

3.1 Microstructure and phase characterization

The microstructures of T3, TX31 and TX32 both in as-cast condition and after extrusion are presented in Figs.1−3 in the same magnification. It can be clearly seen that after extrusion in the binary T3 alloy newly recrystallized fine grains have developed. The average grain size of T3 in as-cast condition (Fig.1(a)) is 345 μm, while the grain size decreases by about 5 times to 64 μm after extrusion (Fig.1(b)).

The grain structure in the ternary alloy TX31 in the cast condition (Fig.2(a)) shows large grains having irregular boundaries, with an average grain size of 520 μm. Though the cast structure has disappeared completely (Fig.2(b)), as in the binary alloy, uniform and clear grain structure has not emerged after extrusion of this alloy. The microstructure reveals the typical fibre-like flow with some recrystallized grains, suggesting

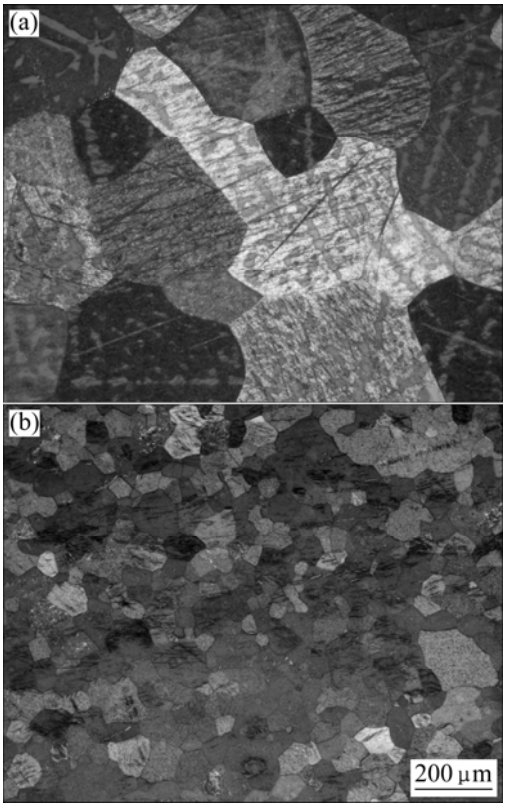

Fig.1 Microstructures of T3-alloy: (a) In as-cast condition; (b) After extrusion

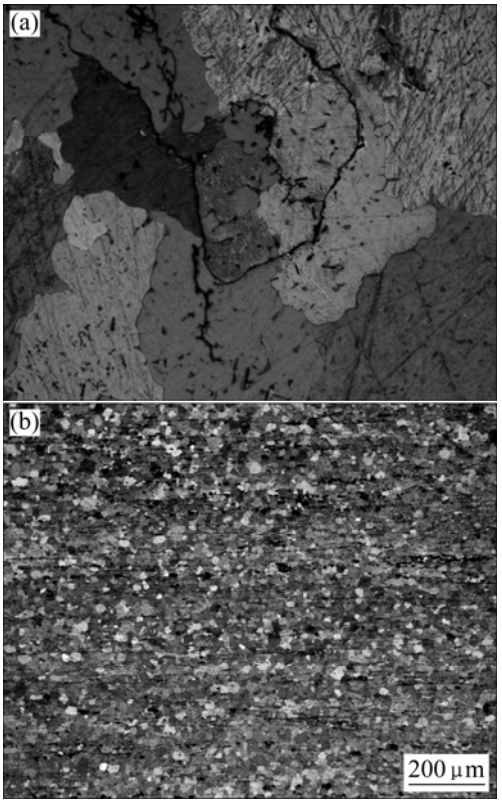

Fig.3 Microstructures of TX32 alloy: (a) In as-cast condition; (b) After extrusion

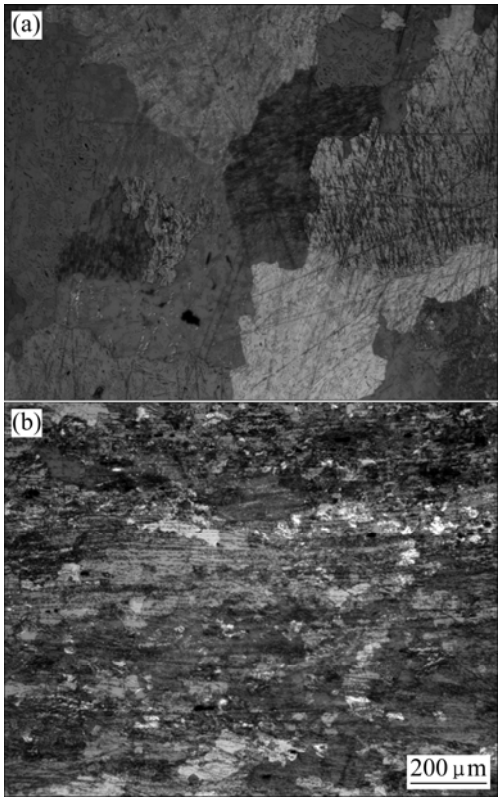

Fig.2 Microstructures of T31 alloy: (a) In as-cast condition; (b) After extrusion

inadequate temperature conditions for full dynamic recrystallization.

The microstructure of cast TX32 alloy (Fig.3(a)) is somewhat similar to TX31 alloy except that the grain is slightly smaller at 455 μm and has smooth grain boundaries. The microstructure of the extruded material (Fig.3(b)) has shown very fine grains of uniform size, with an average grain size of 18 μm. This shows a fully recrystallized microstructure.

XRD measurements detect several phases in these alloys. The very few phases observed in both as-cast and extruded conditions of the binary T3 alloy have been identified as Mg_2Sn. However, in the ternary TX31 alloy only the $Ca_{2-x}Mg_xSn$ phase has been identified. On the other hand, in the TX32 alloy the Mg_2Ca phase has been detected besides the $Ca_{2-x}Mg_xSn$ phase. Earlier studies [11−19] have indicated similar results with the presence of Mg_2Ca phase predominantly at the grain boundaries. It is proposed that existing Ca and Sn will be first used to develop the particles of $Ca_{2-x}Mg_xSn$ type and the remaining amounts of Ca will eventually form the Mg_2Ca phase. Formation of Mg_2Sn and Mg_2Ca phases can be expected on the basis of the respective binary phase diagrams of Mg-Sn and Mg-Ca systems[24] depending on the amount of alloying elements added. A summary of the phases identified and grain size of the

alloys in both as-cast and extruded conditions is given in Table 2. It may be proposed that Mg_2Ca phase distributed at the grain boundaries is largely responsible for the development of fine recrystallized grains in the case of TX32 alloy.

Table 2 Phases found and grain sizes in as-cast condition and after extrusion of selected alloys

Alloy	Phases detected using XRD	Average grain size/μm	
		As-cast	Extruded
T3	Mg_2Sn	345	64
TX31	$Ca_{2-x}Mg_xSn$	520	34*
TX32	$Ca_{2-x}Mg_xSn$, Mg_2Ca	455	18

* Grain was not uniformly recrystallized.

3.2 Corrosion behavior

The results of corrosion tests are given in Table 3 for T3, TX31 and TX32 obtained from potentio-dynamic polarization and salt spray tests. While the free potential is within a narrow range for all the alloys in as-cast and extruded conditions, there are significant differences in the corrosion rates between as-cast and extruded conditions of all the alloys. The corrosion resistance of the alloys increases enormously after extrusion and reaches values closer to those of a highly corrosion resistant alloy AZ91D. This significant increase can be attributed to reduction in microporosities and segregation, and recrystallization of the original large grains into smaller ones that have been accomplished due to extensive hot working of the alloys. The results of salt spray test of the extruded alloys also follow similar trend to that observed in potentio-dynamic polarization tests. However, the behavior might be related to the phases present which are similar and more uniformly distributed after extrusion. The phases can form micro-galvanic cells on the specimen surface, thus enhancing the corrosion attack. Looking at the measured corrosion rates and the phases detected in the various alloys, one can assume that Mg_2Sn is less detrimental for the surrounding magnesium matrix than $Ca_{2-x}Mg_xSn$. Latter is still better than the mixture of $Ca_{2-x}Mg_xSn$ and Mg_2Ca. However, more electrochemical studies of the single phases are required and will be performed to give a final answer.

Table 3 Corrosion rates of selected alloys in as-cast condition and after extrusion

Alloy	Condition	Free potential (polarization test)/mV	Corrosion rate/mm	
			Polarization test	Salt spray test
Mg-3Sn	As-cast	−1 364.8±14.8	1.41±0.62	1.65±0.05
	Extruded	−1 363.5±4.0	0.80±0.13	1.50±0.21
Mg-3Sn-1Ca	As-cast	−1 366.6±11.7	2.07±0.31	2.34±0.21
	Extruded	−1 391.4±2.1	1.76±0.08	1.91±0.40
Mg-3Sn-2Ca	As-cast	−1 403.6±5.2	5.92±0.23	5.99±0.44
	Extruded	−1 392.0±2.5	3.14±0.08	2.28±0.16
AZ91D [27]	As-cast	−1343.0±6.4	0.43±0.04	1.07±0.23

4 Conclusions

1) The corrosion behavior of three cast and extruded Mg-alloys, based primarily on binary Mg-3Sn system with addition of Ca in the range of 1%−2%, have been investigated using polarization and salt spray test methods.

2) Studies on the microstructure of the selected alloys using OM and XRD facility have revealed that the alloys retain the original second phases found in their cast condition, such as Mg_2Sn, Mg_2Ca and $Ca_{2-x}Mg_xSn$. However, the grain size has significantly reduced due to the occurrence of extensive recrystallization in the extrusion process.

3) The corrosion resistance of the three alloys has improved after extrusion compared with the same alloys in their as-cast condition. The corrosion resistance of extruded materials is comparable to AZ91D. Furthermore, the corrosion behavior is influenced by the phases present in the alloys, with Mg_2Sn being the most compatible followed by $Ca_{2-x}Mg_xSn$ and finally Mg_2Ca.

Acknowledgement

The authors would like to thank Dr. J. Bohlen, GKSS Research Centre GmbH Geesthacht for his contribution in the planning and extrusion experiments. Support from City University of Hong Kong through Strategic Research Grant (Project #7002013) is acknowledged.

References

[1] SCHUMANN S. The paths and strategies for increased magnesium applications in vehicles [J]. Mat Sci Forum, 2005, 488/489: 1−8.

[2] WESTENGEN H, BAKKE P, ALBRIGHT D A. Advances in magnesium alloy development [C]// Proc. 61st Annual World Magnesium Conference 2004. New Orleans, Louisiana, USA, 2004: 33−44.

[3] AGHION E, BRONFIN B, FRIEDRICH H. The environmental impact of new magnesium alloys on the transportation industry [C]// Magnesium Technology 2004. TMS, 2004: 167−172.

[4] LUO A A. Recent magnesium alloy development for powertrain applications [J]. Mat Sci Forum, 2003, 419/422: 57−66.

[5] HAN Q, KAD B K, VISWANATHAN S. Design perspectives for creep-resistant magnesium die-casting alloys [J]. Phil Mag, 2004, 84: 3843−3860.

[6] DARGUSCH M S, DUNLOP G L, PETTERSEN K. Elevated temperature creep and microstructure of die cast Mg-Al alloys [C]// Magnesium Alloys and their Applications. Werkstoff-Informations GmbH, Wolfsburg, Germany, 1998: 277−282.

[7] BAKKE P, WESTENGEN H. Die casting for high performance—Focus on alloy development [J]. Adv Eng Mat, 2004, 5: 879−885.

[8] PEKGULERYUZ M O, LABELLE P, BARIL E, ARGO D. Magnesium diecasting alloy AJ62x with superior creep resistance [C]// Magnesium Technology 2003. TMS, 2003: 201−206.

[9] PEKGULERYUZ M O, KAYA A A. Magnesium die casting alloys for high temperature applications [C]// Magnesium Technology 2004. TMS, 2004: 281−287.

[10] BARIL E, LABELLE P, FISCHERSWORRING-BUNK A. AJ (Mg-Al-Sr) alloy system used for new engine block [R]. SAE Technical Paper Series 2004-01-0659.C.

[11] BOWLES A L, BLAWERT C, HORT N, KAINER K U. Microstructural investigations of the Mg-Sn and Mg-Sn-Al alloy systems [C]// LUO A A, ed. Magnesium Technology 2004. TMS, 2004: 307−310.

[12] BOWLES A L, DIERINGA H, BLAWERT C, HORT N, KAINER K U. Investigations in the magnesium-tin system [J]. Mat Sci Forum, 2004, 488/489: 135−138.

[13] KOZLOV A, OHNO M, ABU LEIL T, HORT N, KAINER K U, SCHMID-FETZER R. Phase equilibria and thermodynamics of the Mg-Sn-Ca system (Part 2): Experimental investigation of ternary Mg-Sn-Ca phase equilibria and solidification microstructure [J]. Intermetallics, 2008, 16: 316−321.

[14] HORT N, RAO K P, ABU LEIL T, DIERINGA H, PRASAD V Y R K, KAINER K U. Creep and hot working behaviour of a new magnesium alloy Mg-3Sn-2Ca [C]// Magnesium Technology 2008. TMS, 2008: 401−406.

[15] ABU LEIL T, RAO K P, HORT N, HUANG Y, BLAWERT C, DIERINGA H, KAINER K U. Microstructure, corrosion and creep of cast magnesium alloys Mg_2Sn_2Ca and Mg_4Sn_2Ca [C]// Magnesium Technology 2007. Orlando: TMS, 2007: 257−262.

[16] KAINER K U, RAO K P, HUANG Y, ABU LEIL T, HORT N. Properties and processing of new magnesium-tin-calcium alloys for powertrain and hand tool applications [C]// ICM 2007. Chongqing, China, 2007.

[17] ABU LEIL T, HUANG Y, DIERINGA H, HORT N, KAINER K U, BURŠÍK J, JIRÁSKOVÁ Y, RAO K P. Effect of heat treatment on the microstructure and creep behavior of Mg-Sn-Ca alloys [C]// International Conference on Magnesium. ICM 2006, Beijing, China, 2006.

[18] BURŠÍK J, ZÁBRANSKÝ K, JIRÁSKOVÁ Y, BURŠÍKOVÁ V, ABU LEIL T, BLAWERT C, HUANG Y, DIETZEL W, HORT N, KAINER K U, RAO K P. Effect of heat treatment on the microstructure, microhardness and corrosion behavior of cast Mg-3Sn-2Ca alloy [C]// Magnesium Alloys and their Applications. Werkstoff-Informations GmbH, Dresden, Germany, 2006: 49−54.

[19] BURŠÍK J, ZÁBRANSKÝ K, JIRÁSKOVÁ Y, BURŠÍKOVÁ V, ABU LEIL T, BLAWERT C, HUANG Y, DIETZEL W, HORT N, KAINER K U, RAO K P. Microstructure and micromechanical properties of as-cast Mg-Sn-Ca and Mg-Sn-Mn alloys [C]// Magnesium Alloys and their Applications. Werkstoff-Informations GmbH, Dresden, Germany, 2006: 37−42.

[20] ABU LEIL T, RAO K P, HORT N, BLAWERT C, KAINER K U. Corrosion behaviour and microstructure of a broad range of Mg-Sn-X alloys [C]// Magnesium Technology 2006. San Antonio: TMS, 2006: 281−286.

[21] HORT N, HUANG Y, ABU LEIL T, MAIER P, KAINER K U. Microstructural investigations of the Mg-Sn-*x*Ca system [J]. Adv Eng Mat, 2006, 8: 359−364.

[22] MENDIS C L, BETTLES C J, GIBSON M A, HUTCHINSON C R. An enhanced age hardening response in Mg-Sn based alloys containing Zn [J]. Mat Sci Eng A, 2006, 435/436: 163−171.

[23] LIU H, CHEN Y, TANG Y, HUANG D, NIU G. The microstructure and mechanical properties of permanent-mould cast Mg-5wt%Sn-(0−2.6)wt%Di alloys [J]. Mat Sci Eng A, 2006, 437: 348−355.

[24] NAYEB-HASHEMI A A. Phase diagrams of binary magnesium alloys [M]. ASM International, Ohio, USA: Metals Park, 1998.

[25] BECK A. Magnesium und seine legierungen [M]. Berlin, Germany: Julius Springer Verlag, 1939. (in German)

[26] LUO A A, BALOGH M P, POWELL B P. Creep and microstructure of magnesium-aluminum-calcium based alloys [J]. Metall Mater Trans, 2002, 33A: 567−574.

[27] MORALES E D, BLAWERT C, DIETZEL W, KAINER K U, SCHARF C, DITZE A. Corrosion behaviour of a new AZ based secondary alloy with improved tolerance limits against impurities [C]// Magnesium Alloys and their Applications. Werkstoff Informations GmbH, Dresden, Germany, 2006.

(Edited by YANG Bing)